Application of ONIOM calculations in the study of the effect of the zeolite framework on the adsorption of alkenes to ZSM-5

Supawadee Namuangruk [a], Duangkamol Tantanak [b], Jumras Limtrakul [a,*]

[a] *Laboratory for Computational and Applied Chemistry, Chemistry Department, Faculty of Science, Kasetsart University, Bangkok 10900, Thailand*
[b] *Chemistry Department, Faculty of Science, King Mongkut's Institute of Technology, Ladkrabang, Bangkok 10520, Thailand*

Abstract

The structures and energetics associated with the adsorption of ethene and four butene isomers on H-ZSM-5 zeolite have been studied using a 46T cluster and calculated at the ONIOM2(B3LYP/6-311++G(d,p):UFF) level. The adsorption energy for ethene-zeolite complex is predicted to be −8.17 kcal/mol, which is in good agreement with the experimental data of −9.0 kcal/mol. The trend of the calculated adsorption energies (kcal/mol) for the butene isomers is as follows: 1-butene (−16.06) > *cis*-2-butene (−13.62) ≅ *trans*-2-butene (−13.25) > isobutene (−6.96). The isobutene–zeolite complex is the least stable due to the greatest steric repulsion between the methyl substituents around the C═C bond and zeolite framework; the more substituted the lower the adsorption energy. Although our own N-layered integrated molecular orbital and molecular mechanics (ONIOM) calculation results indicate that isobutene hardly approaches the acid site and has a weak interaction with the zeolite framework, NBO analysis shows that it has the maximum charge transfer from the active site and the largest stabilization energy. These findings explain the reason why ZSM-5 is selective towards isobutene produced from *n*-butene and indicate that the acidic proton from the zeolite is easy to transfer to isobutene. Thus, further catalytic conversion of isobutene would be facile.
© 2006 Elsevier B.V. All rights reserved.

Keywords: Butene; Adsorption; Zeolite; ZSM-5; ONIOM

1. Introduction

Isobutene is an important industrial chemical that is produced during the fractionation of refinery gases. The primary uses of isobutene are in the production of polymers such as diisobutylene, isobutylene trimers, butyl rubber, and others through skeletal isomerization [1–11]. Skeletal isomerization of isobutene is of considerable interest currently as it is a commercially important precursor to methyl tertiary butyl ether (MTBE), an octane enhancing fuel additive demanded worldwide for use in cleaner burning gasoline. Traditionally, isobutene is produced from the catalytic cracking of hydrocarbons in oil refineries; however, these sources cannot meet the increased demand. Consequently there is an increasing interest in the isomerization of the much more abundant linear butenes as a new source of this branched olefin.

Several experimental studies [10–15] have shown that zeolites of medium pore size are excellent catalysts for the skeletal isomerization of isobutene. Zeolites containing 10-membered ring small-pores such as ferrierite, ZSM-5, ZSM-22, ZSM-57, MCM-22, have been shown to exhibit high selectivity for skeletal isomerization of butene isomers [9,16–18]. ZSM-5, for example, is found to be a quite promising catalyst, amongst others, with high selectivity toward isobutene [18]. Its selectivity has been assumed to be a result of two main factors: (1) the medium strength acidity which primarily affects the activity and (2) the medium pore size, which allows skeletal isomerization of linear butenes and minimizes oligomerization, possibly as a result of steric constraints and/or diffusion effects [19–24].

The adsorption of butene isomers to the acidic zeolite site is the starting point for any study of the skeletal isomerization of butenes. In this present paper we investigate the influence of the topology of zeolite ZSM-5 on the adsorption of the four butene isomers, using the combination of quantum mechanics and molecular mechanics. We also compare our results obtained in the presence and absence of the zeolite framework to deter-

* Corresponding author. Tel.: +66 29428900x323; fax: +66 29428900x324.
E-mail address: fscijrl@ku.ac.th (J. Limtrakul).

mine how significant the adsorption is affected by the steric constraints of the pore.

The goal of this study is to help the elucidation of the reasons behind butene selectivity in ZSM-5 zeolite catalysts. Here, we focus on the first step of this process, adsorption of the substrates to the zeolite which must occur prior to the catalytic reaction. We employ the ONIOM methodology to model the 46T zeolite–substrate system as this allows us to represent this large, complicated system at a reasonable computational price. In recent studies the ONIOM model has been successfully employed to study the adsorption of ethene, benzene and ethylbenzene over acidic faujasite and ZSM-5 zeolites [25–28] giving us confidence in the method. The models used here consist of an inner-layer of active region modeled by a small cluster using density functional theory to account for the interactions of the adsorbates with the acid site of zeolite, and a large outer-layer of the zeolite framework represented by a molecular mechanics force field to account for the van der Waals interactions due to confinement of the microporous structure [6,25,26,29–33].

2. Computational procedure

We have employed two different ONIOM strategies to investigate four isomers of butene, 1-butene, *cis*-2-butene, *trans*-2-butene, and isobutene in ZSM-5, in an effort to understand its selective nature. In our previous study [26], the ONIOM methods obviously showed a compromise between an accurate treatment of the active site core and the zeolite framework as well as the computational resource and time consumption. However, it should be noted that the accuracy of this method depends significantly on the choice of the level of calculations for the inner- and outer-layers. To ensure the core and framework were properly treated we considered two different models (Fig. 1). In the first models (Fig. 1a), which we term the ONIOM2 model, a moderately sized active site region (represented with balls and sticks) is described using a high-level of theory, and the extended framework (represented by lines) considered using a low-level. The second model (Fig. 1b), which we term the ONIOM3 model, consists of a smaller representation of an active site region (represent by balls and sticks) treated at the high-level, and the intermediate region (represent by sticks) treated at the medium-level approach and the framework (represented by lines) treated using a low-level.

The total energies of the ONIOM2 and ONIOM3 systems can be expressed within the framework of the ONIOM methodology developed by Morokuma and his co-worker [34].

$$E_{\text{ONIOM2}} = E_{\text{Low}}^{\text{Real}} + (E_{\text{High}}^{\text{Cluster}} - E_{\text{Low}}^{\text{Cluster}}),$$

$$E_{\text{ONIOM3}} = E_{\text{Low}}^{\text{Real}} + (E_{\text{Medium}}^{\text{Intermediate}} - E_{\text{Low}}^{\text{Intermediate}}) - (E_{\text{High}}^{\text{Cluster}} - E_{\text{Medium}}^{\text{Cluster}})$$

where the superscripts *Real*, *Intermediate*, and *Cluster* mean the whole system, the intermediate layer, and the active site region, respectively. Subscripts *Low*, *Medium*, and *High* mean low-, medium-, and high-level methodologies used in the ONIOM calculations.
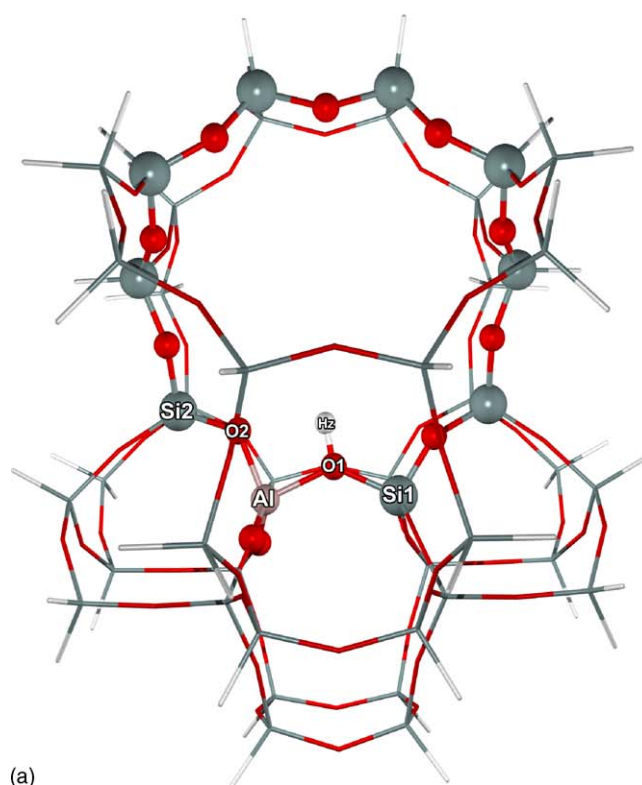
(a)
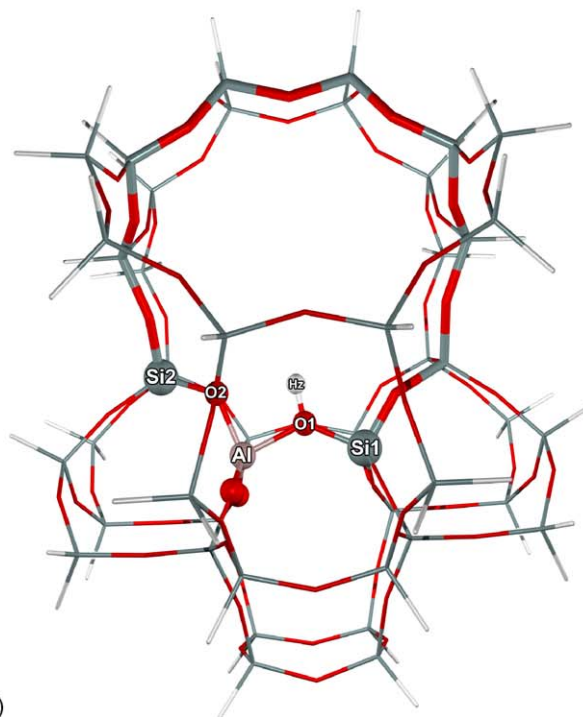
(b)

Fig. 1. The ONIOM2 (a) and ONIOM3 (b) layers of the 46T model of H-ZSM-5; balls and sticks represent the high layer, sticks represent the medium layer and lines represent the low layer.

The zeolitic structures used in this study were modeled as follows: for the ONIOM2 system, a 10T ring core region of H-ZSM-5 zeolite was modeled at the B3LYP/6-31G(d,p) level while the remainder is treated using the universal force field (UFF)

of Rappe et al. [35], ONIOM2(B3LYP/6-31G(d,p):UFF). This system was optimized in the presence of the four substrates. We subsequently reoptimized the cluster using a further ONIOM3 system where the core is separated into two parts. One, the 3T region, [≡SiO(H)Al(O)₂OSi≡], the representation of an active site calculated at the MP2/6–31G(d,p) level, and two, the 7T ring fragment connecting the 3T acidic site to complete the 10T pore opening of the ZSM-5 zeolite is treated with the HF/3–21G method. The rest of the extended framework is also treated with the UFF force field, ONIOM3(MP2/6–31G(d,p):HF/3-21G:UFF).

All results are obtained from calculations by using the Gaussian03 code [36]. During the structure optimization, only the active site region [≡SiO(H)Al(O)₂OSi≡], and the adsorbates are allowed to relax. The single-point energy calculations at the ONIOM2(B3LYP/6-311++G(d,p):UFF)//ONIOM2(B3LYP/6-31G(d,p):UFF) and ONIOM3(MP2/6-311++G(d,p):HF/6-31G(d):UFF)//ONIOM3(MP2/6-31G(d,p): HF/3-21G:UFF) levels are also carried out to obtain more reliable energies.

The interaction between a butene molecule and an acidic site was analyzed by the natural bond orbital analysis (NBO) [37]. The energetic stabilization due to donor–acceptor interactions can be estimated by the second-order perturbation theory:

$$\Delta E_{\sigma \to \sigma*}^{(2)} = -2 \frac{\left\langle \sigma | \hat{F} | \sigma* \right\rangle^2}{\varepsilon_{\sigma*} - \varepsilon_{\sigma}}$$

where σ is the filled (donor) orbital, $\sigma*$ is the unfilled (acceptor) orbital, $\hat{F}$ the Fock operator, and ε_{σ} and $\varepsilon_{\sigma*}$ are the NBO orbital energies of donor and acceptor orbitals. The quantity of charge q transferred associated with $\sigma \to \sigma*$ interactions between donor and acceptor orbitals is:

$$q \cong \frac{|\Delta E_{\sigma \to \sigma*}^{(2)}|}{\varepsilon_{\sigma*} \to \varepsilon_{\sigma}}$$

($\sim 10^{-3}$ e) which is typically much less than that required for formation of an ion pair.

3. Results and discussion

3.1. Active site models

Two different ONIOM schemes, ONIOM2 and ONIOM3, have been performed as the zeolite models for the study of butene/zeolite adsorption complexes. The important geometric parameters of the two models are listed in Table 1. It is seen that, geometric parameters for the ONIOM2 structure, the active site of which contains 10T atoms (calculated by B3LYP), is slightly different from those for the ONIOM3 structure where the active site is separated into a 3T region (calculated by MP2) and connecting 7T atoms (calculated by HF). Indeed, the ONIOM3 structure shows the shorter bond distance, Al–O1, Al–O2, Si–O1, and Si–O2, than the ONIOM2 structure.

The supporting information for the reliability of the active site is given from the NMR studies. Klinowski and his co-workers [38] have estimated the internuclear distance between aluminum and proton nuclei in a Brønsted acid site, r(Al···H), of H-ZSM-

Table 1
The optimized geometric parameters of ONIOM2 and ONIOM3

	ONIOM2	ONIOM3
Distances		
O1–Hz	0.970	0.971
Al–Hz	2.307	2.345
Al–O1	1.855	1.852
Al–O2	1.669	1.665
Si1–O1	1.658	1.651
Si2–O2	1.584	1.579
Angles		
∠O1–Al–O2	86.02	85.65
∠Al–O1–Si1	135.70	135.22
∠Al–O2–Si2	118.90	119.33

Distances are in angstroms and angles are in degrees.

5 to be 2.48 ± 0.04 Å. Our calculations have shown that the Al–Hz distance for the ONIOM3 of 2.345 Å gives more comparable results to experimental data than that for the OMIOM2 of 2.307 Å. However, the O–Hz bond lengths of both structures are nearly identical. Therefore, we use both ONIOM2 and ONIOM3 structures as the zeolite models for the further study of butene/zeolite adsorption complexes.

3.2. Adsorption structures

Theoretical studies [39,40] indicated that the relative stability of the complex formed by the adsorption of the two butene isomers on the bare zeolite cluster is; 1-butene > isobutene. However, these results were based on gas phase clusters, so it is not clear how the crystalline framework of the zeolite will affect the adsorption process. Therefore, to justify this point, we included the zeolite framework effect via the ONIOM method.

The optimized structures for the adsorption of the zeolite–butene complexes are illustrated in Fig. 2. It is noted that the adsorption of olefins on zeolite can be isomerization at the active site where the Brønsted acid proton interacts with the C=C double bond of olefins [13]. The acidic proton in zeolite points to the centre of the C=C double bond, resulting in the lengthening of the C=C bond as a consequence of the weakening of the π bond of the olefins and the O–Hz bond of zeolite. This phenomenon can be described by the charge transfer and stabilization energy between alkenes and zeolite (Table 2), which are calculated by NBO analysis [37] (cf. Fig. 2). For all of the butene isomers adsorbed on the Brønsted acid of zeolite, NBO calculations show that there are modes of charge q transfer due to the orbital interaction between the π bonding (donor) orbital of the C=C bond of butene with the σ* antibonding (acceptor) orbital of O–Hz bond of zeolite. The stabilization energies of these modes are proportional to the quantity of charge q transferred; the more charge transferred the larger stabilization energies.

Table 2 shows the trend of quantity of charge transferred associated with the interaction between the $\pi_{C=C}$ and the $\sigma*_{O-Hz}$ orbitals; isobutene (0.013) > 1-butene (0.012) > cis-2-butene (0.009) > trans-2-butene (0.003), which corresponds to the trend of the associated stabilization energy: isobutene (5.23) > 1-butene (5.04) > trans-2-butene (3.76) > cis-2-butene (1.26), and
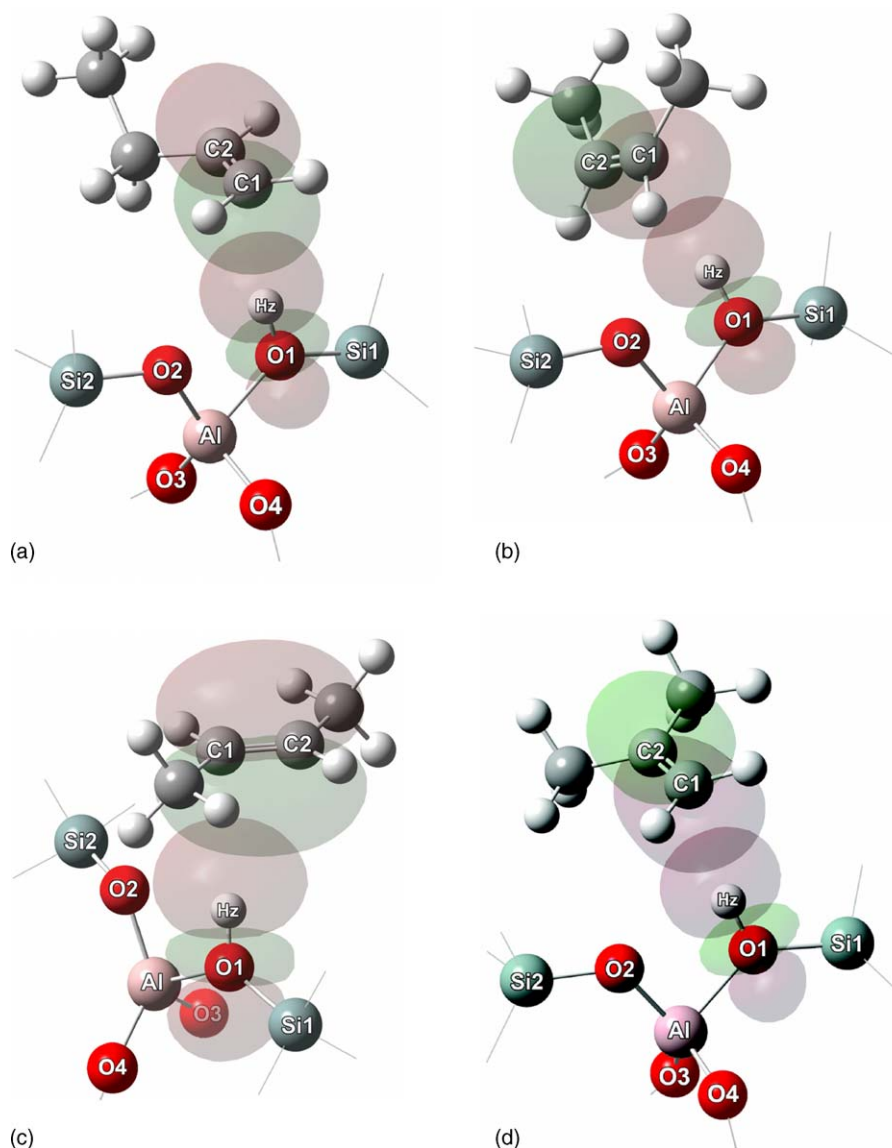
Fig. 2. Overlapping between the π bonding orbital of C1=C2 and σ^* antibonding orbital of O–Hz for adsorption complexes of zeolite with (a) 1-butene; (b) *cis*-2-butene; (c) *trans*-2-butene; (d) isobutene.

the net charge transfer determined by NPA in the butene molecule: isobutene (0.02452) > 1-butene (0.02439) > *trans*-2-butene (0.01664) > *cis*-2-butene (0.00713). Moreover, we also found that these results correspond to the trend of the shortest C···Hz distances; isobutene (2.303) > 1-butene (2.384) > *cis*-2-butene (2.425) > *trans*-2-butene (2.487) (see Table 3b). These

findings indicate that the alkene which is closer to the acidic proton of zeolite would prefer the charge transfer and result in the higher stabilization energy.

The fact is that, the less the bond order the longer the bond distance and vice versa, and the causes of the reducing of the bond order are: (1) the loss of electron occupancy in the bonding

Table 2

The NBO analysis represented the magnitude of transferred electron and stabilization energy for butene isomers adsorbed on a 46T cluster model calculated at ONIOM2(B3LYP/6-31G(d,p):UFF)

ONIOM2	1-Butene	*trans*-2-Butene	*cis*-2-Butene	Isobutene
Electron transfer[a]	0.01205	0.00301	0.00930	0.01290
Stabilization energy[b] (kcal/mol)	5.04	1.26	3.76	5.23
Net charges[c]	0.02439	0.00713	0.01664	0.02452

[a] Electron density transfer from the π bonding of the C=C bond of butene to σ^* antibonding of O–Hz of zeolite.

[b] The stabilization energy due to the mode of electron transfer from the π bonding of the C=C bond of butene to σ^* antibonding of O–Hz of zeolite.

[c] Net charge transfer determined by NPA in butene molecule.

Table 3

Optimized geometric parameters of alkenes of the 46T cluster model calculated at (a) ONIOM2(B3LYP/6-31G(d,p):UFF) level and (b) ONIOM3(MP2/6-31G(d,p):HF/3-21G:UFF)

	Ethene	1-Butene	*trans*-2-Butene	*cis*-2-Butene	Isobutene
Part (a)					
Distances					
C1=C2	1.341	1.344	1.346	1.348	1.344
C1–Hz	2.303	2.335	2.313	2.403	2.241
C2–Hz	2.348	2.347	2.358	2.490	2.641
O1–Hz	0.981	0.985	0.987	0.981	0.984
C2–O2	3.310	3.462	3.072	3.196	3.562
Al–O1	1.837	1.835	1.834	1.835	1.836
Al–O2	1.664	1.663	1.663	1.661	1.665
Si1–O1	1.647	1.649	1.649	1.650	1.649
Si2–O2	1.573	1.572	1.571	1.571	1.573
Angles					
∠Al–O1–Hz	111.93	111.97	112.06	112.35	112.34
∠Al–O2–C2	111.07	113.52	122.40	116.60	117.91
∠O2–C2–C1	71.75	65.13	94.08	72.99	69.61
∠O1–Al–O2	86.50	86.50	86.60	86.80	86.40
∠Si1–O1–Al	120.90	133.00	132.60	133.10	133.10
∠Si2–O2–Al	134.00	120.90	121.20	121.40	120.30
Part (b)					
Distances					
C1=C2	1.335	1.338	1.340	1.343	1.342
C1–Hz	2.433	2.384	2.487	2.425	2.303
C2–Hz	2.524	2.671	2.590	2.621	2.806
O1–Hz	0.978	0.981	0.981	0.981	0.983
C2–O2	3.734	3.850	3.674	3.319	3.712
Al–O1	1.843	1.839	1.839	1.839	1.843
Al–O2	1.668	1.667	1.665	1.664	1.667
Si1–O1	1.654	1.655	1.656	1.656	1.655
Si2–O2	1.578	1.576	1.576	1.576	1.576
Angles					
∠Al–O1–Hz	109.31	109.52	109.58	109.93	109.06
∠Al–O2–C2	109.68	111.78	114.17	116.17	117.81
∠O2–C2–C1	69.98	60.08	70.26	70.57	63.97
∠O1–Al–O2	86.70	86.80	87.00	87.10	86.80
∠Si1–O1–Al	120.30	133.70	133.70	133.70	133.80
∠Si2–O2–Al	134.40	120.10	120.30	121.00	120.50

Distances are in angstroms and angles are in degrees.

orbital and (2) the gain in electron occupancy in the antibonding orbital. We can explain the elongation of the O–Hz and C=C bonds in butene adsorption complex on account of the σ* antibonding orbital of the O–Hz bond. It is partially filled by electrons from the π bonding orbital of C=C bond of butene; the less the bond order, the longer the O–Hz and C=C bonds. These observations are confirmed by the geometric parameters in Table 3a and b.

The optimized geometric parameters of the butene isomers over the 46T cluster model of ZSM-5 zeolite are calculated by using both the ONIOM3(MP2/6-31G(d,p):HF/3-21G:UFF) and the ONIOM2(B3LYP/6-31G(d,p):UFF) methods (Fig. 3 and Table 3a and b). The obtained results show that the smaller the alkyl groups around the C=C bond, which will result in less steric hindrance, the greater the association with the zeolite acid site. This manifests itself in terms of shorter C···Hz distance and a longer C=C bond in the butene. In general, we see the same trends at both levels of theory, with the most significant

difference relating to the C···Hz distances. At the ONIOM3 level, these distances are maintained at a similar length, unlike at the ONIOM2 level where they differ more significantly. An exception of this is isobutene, which is a result of unfavorable steric effects.

For 1-butene, *cis*- and *trans*-2-butenes, the sp^2 hybridized carbon atoms of olefins and the atoms or groups attached to these carbons all lie in the same plane. Isobutene, on the other hand, must lie at right angles to the plane adopted by the other three isomers in order to minimize unfavourable steric contact. At both levels of theory, the C=C bonds of the substrates are found to be slightly elongated compared to those in the isolated gas phase substrate in the following decreasing order: 1-butene > *trans*-2-butene > *cis*-2-butnene ≈ isobutene. For the ONIOM2 level, we see a corresponding increase in the average C···Hz distances (C1···Hz and C2···Hz) where the distances follow the following trend: 1-butene ≅ *trans*-2-butene < *cis*-2-butene ≅ isobutene.
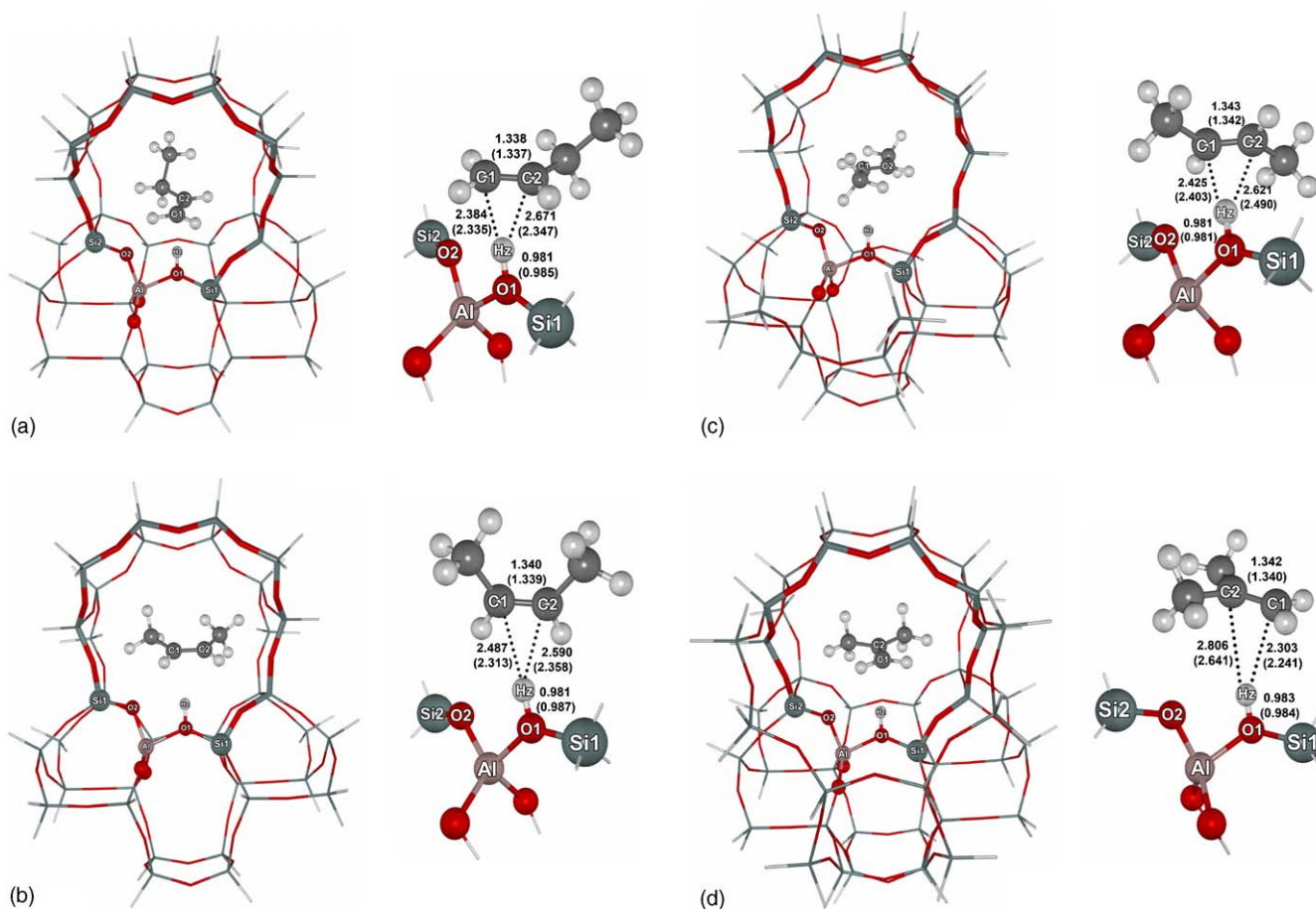
Fig. 3. The optimized structures of (a) 1-butene; (b) *cis*-2-butene; (c) *trans*-2-butene; (d) isobutene on the active site of 46T models calculated by using ONIOM2(B3LYP/6-31G(d,p):UFF). The numbers in parentheses are calculated by using ONIOM3(MP2/6-31G(d,p):HF/3-21G:UFF).

In all cases, the zeolite O–Hz distance is elongated; however, surprisingly it is more so with isobutene. Furthermore, while isobutene hardly approaches the zeolite, it has the shortest Hz···C distance and one of the longest O–Hz distances, but the largest stabilization energy and the most charge transfer. This seems to indicate that proton transfer from the zeolite to isobutene would be more facile, thus making its catalytic conversion more facile.

The geometric parameters of butene isomers on the active site of the 46T models calculated using ONIOM2 and ONIOM3 methods are found to be significantly altered compared to those in 3T zeolite clusters calculated elsewhere [41,42]. This specifically relates to the conformation of the substrates relative to the zeolite, where the greater conformational freedom leads to less realistic structures. These include the elongation of the C=C bonds and the O–Hz bonds. This indicates that the framework is important in defining the conformation of binding for specific substrates. However, the optimized parameters of the C=C bonds of the adsorbed butenes and of the O–Hz groups in the π-complex are similar to those in isolated butene. The key similarities are that the C=C bond of any substrate will be lengthened slightly on account of the increased overlap between the π bonding orbitals of the alkenes and the O–Hz bonding orbital of acidic zeolite. The C1···Hz and C2···Hz bonds are expected to be nearly identical for ideally bound substrates, which implies that the interaction between the acidic proton and both carbon atoms is symmetric (Fig. 3). Furthermore, the elongation of the zeolitic proton O–Hz bond will make transfer of a proton to the substrate more facile [43,44], thereby allowing the catalytic reaction to proceed.

3.3. Adsorption energies

The adsorption energy is one of the most valuable data obtained from experimental observation which can be used to validate the theoretical data. Unfortunately, butene rapidly oligomerizes on H-ZSM-5 catalyst even at room temperature [45]. Thus, the adsorption energy could not so far be measured. It has been reported that the experimental data of ethene adsorption on H-faujasite zeolite is −9.0 kcal/mol [46]. However, we calculated the ethylene/H-ZSM-5 adsorption energy of −8.17 kcal/mol, slightly lower than expected due to H-ZSM-5 zeolite being generally more acidic than H-faujasite.

The further supporting result was found from molecular dynamics (MD) simulations [6]. Jousse et al. predicted that adsorption energies for butene isomers adsorption on silicalite zeolite are indistinguishable, but give the trend as follows: 1-butene (−44.7 kJ/mol) > *trans*-2-butene (−43.6 kJ/mol) ≅ *cis*-

2-butene (−43.4 kJ/mol) > isobutene (−39.3 kJ/mol). In addition, the adsorption energy of ethene, 1-butene and isobutene evaluated from gas phase QM calculations carried out by Boronat et al. [41] are also predicted to be −6.14 kcal/mol for ethene, −8.24 kcal/mol for 1-butene and −5.62 kcal/mol for isobutene. It is rather small, which may be due to the small zeolite cluster size used. Recently, Nieminen et al. [47] have reported the adsorption energy of ethene, 1-butene and isobutene by using a hybrid QM/MM study. Their adsorption energies are −8.61, −10.77, and −9.81 kcal/mol for ethene, 1-butene and isobutene, respectively.

In this study, the adsorption energies of the four butene isomers: 1-butene, *trans*-2-butene, *cis*-2-butene and isobutene can be differentiated by the ONIOM2 calculations. The trend of the calculated adsorption energies for butene isomers is: 1-butene (−16.60 kcal/mol) > *trans*-2-butene (−13.25 kcal/mol) $\cong$ *cis*-2-butene (−13.62 kcal/mol) > isobutene (−6.96 kcal/mol). These results are comparable to the ethene adsorption energy of −8.17 kcal/mol and give the same trend as earlier studies.

Comparison between the ONIOM2 and the ONIOM3 calculations are also taken into account. The ONIOM2 adsorption energies are smaller than those of the ONIOM3, which are due to the different methods used in the QM core layer, while the size effects of the framework are identical. Table 4a and b shows the breakdown of the ONIOM adsorption energy for partitioning the energy taken from the QM core and the framework component. The zeolite–ethene adsorption energy from the QM core is only −5.34 kcal/mol, which underestimates the experimental data of −9.0 kcal/mol. The more reliable results are attained when the framework component energy is taken into account (−10.77 kcal/mol). Therefore, the effect of the zeolites framework introduced when the ONIOM method is used is crucial for describing the structure and energetic of the butene adsorption complex. Furthermore, the QM core adsorption energy of ethene (−5.34 kcal/mol) is almost equivalent to that of 1-butene (−5.77 kcal/mol). However, the adsorption energy of ethene and 1-butene can be obviously differentiated in the presence of the framework component in the ONIOM model. More to the point,

the ONIOM scheme suggests that the adsorption energies of *cis*- and *trans*-2-butene are almost equivalent.

1-Butene is predicted to bind to the zeolite more effectively than other butene isomers because it interacts with the zeolite environment more strongly and does not suffer as significantly as the conformational energy penalty on entering the relatively restrictive zeolite cavity as the others. The distortion of the substrates on entering the zeolite is caused by the difference between the gas phase optimal energy and the single point energy of the substrate from the zeolite conformation. The differences are 0.17, 0.16, 0.31 and 1.30 kcal/mol for 1-butene, *trans*-2-butene and *cis*-2-butene and isobutene, respectively. Thus, *trans*-2-butene and *cis*-2-butene are predicted to bind to the zeolite approximately 2–3 kcal/mol less effectively than 1-butene, which can be explained by its weaker interaction with the zeolite environment. Similarly, isobutene is predicted to bind more weakly to the zeolite than to the other substrates formed in the active site at both levels of theory on account of its lower interaction energy with the zeolite environment, which is a result of the high energy distortion conformation. This suggests that the more substituents attached to these small olefins, the more weakly bound they will be.

In summary, the adsorption energy for a butene molecule on a zeolite catalyst arises from the interaction of a butene molecule with the active site and a butene molecule with the zeolite framework as well. For the isobutene molecule, having the most steric hindrance makes it hard to be reoriented to approach the acidic site while being the smallest in an accessible shape causes a small van der Waals interaction with the zeolite framework. On the other hand, the information from the NBO analysis (Table 1) shows the charge transfer from the π bonding (donor) orbital in the C=C bond of the isobutene molecule to the σ* antibonding (acceptor) orbital of O–Hz bond of zeolite. Even though it possesses the smallest adsorption energy, the isobutene molecule delivers the highest electron population to the zeolite (0.02452 e) which corresponds to the highest stabilization energy (5.23 kcal/mol) compared to other butene isomers. It could be clarified that in order to minimize an unfa-

Table 4

The adsorption energies (kcal/mol) of alkenes at the 46T cluster model calculated at (a) ONIOM2(B3LYP/6-31G(d,p):UFF) and (b) ONIOM3(MP2/6-31G(d,p):HF/3-21G:UFF) levels

	Ethene	1-Butene	*trans*-2-Butene	*cis*-2-Butene	Isobutene
Part (a)					
ΔE_{ads}	−10.77	−17.14	−15.16	−14.76	−9.23
Breakdown QM core	−5.34	−5.77	−3.94	−4.52	−2.59
Framework	−5.43	−11.37	−11.22	−10.24	−6.34
ΔE_{ads} SP[a]	−8.17	−16.06	−13.25	−13.62	−6.96
Part (b)					
ΔE_{ads}	−13.93	−23.87	−20.93	−20.33	−14.30
Breakdown QM core	−8.95	−13.18	−13.21	−10.24	−8.23
Framework	−4.98	−10.69	−7.72	−10.09	−6.07
ΔE_{ads} SP[b]	−12.72	−22.89	−17.97	−17.97	−12.07

Also shown are the adsorption energies from the core and framework components.

[a] Single point at ONIOM2(B3LYP/6-311++G(d,p):UFF)//ONIOM2(B3LYP/6-31G(d,p):UFF) level.

[b] Single point at ONIOM3(MP2/6-311++G(d,p):HF/6-31G(d):UFF)//ONIOM2(MP2/6-31G(d,p):HF/3-21G:UFF) level.

vorable steric contact, the isobutene molecule must readjust itself with a suitable direction to the acidic proton of zeolite. According to this situation, the C1 atom would prefer to be leaning toward the Hz atom while the C2 atom has to move out from the active site. These provide an asymmetric configuration of the isobutene adsorbed on the active site with small adsorption energy. However, the smallest C1$\cdots$Hz distance (2.303 Å) would enhance the donor–acceptor electron transfer between the isobutene molecule and the zeolite leading to a more electron population on $\sigma^*_{O–Hz}$ orbital and would make isobutene more facile to be protonated, even with the smallest adsorption energy.

4. Conclusions

We have shown that adsorption energies obtained from the calculations using ONIOM3 were found to be higher than those from ONIOM2. The ONIOM2 calculation gives the adsorption energy of the ethene adsorption complex of -8.17 kcal/mol, which is in good agreement with the experimental data of -9.0 kcal/mol. The predicted adsorption energies of the butene isomers are -16.06, -13.62, -13.25, -6.96 kcal/mol for 1-butene, *cis*-2-butene, *trans*-2-butene and isobutene, respectively. The ONIOM method can differentiate the adsorption energies between ethene and 1-butene on zeolite while the QM core layer gives the same adsorption energies. However, the combination of the QM core and the framework component predicts that the adsorption energies of *cis*- and *trans*-2-butenes are the same.

The results from this study show that the framework computed using the ONIOM methodology is crucial in describing the structure and adsorption of butene isomers probed on the zeolite catalyst system. The adsorption energy of isobutene is predicted to be the smallest as compared to the other and this may help to explain the selectivity of ZSM-5 toward isobutene as this substrate is in a destabilized state. This is reinforced by the fact that the isobutene–zeolite complex seems to be in a less active state than the others. This is currently under investigation in our laboratory.

Acknowledgements

References

[1] M. Guisnet, P. Andy, Y. Boucheffa, N.S. Gnep, C. Travers, E. Benazzi, Catal. Lett. 50 (1998) 159–164.
[2] P. Meriaudeau, R. Bacaud, L. Ngoc Hung, A.T. Vu, J. Mol. Catal. 110 (1996) L177–L179.
[3] P. Meriaudeau, V.A. Tuan, N.H. Le, G. Szabo, J. Catal. 169 (1997) 397–399.
[4] G. Seo, H.S. Jeong, J.M. Lee, B.J. Ahn, Stud. Surf. Sci. Catal. 105B (1997) 1431–1438.
[5] M. Guisnet, P. Andy, N.S. Gnep, E. Benazzi, C. Travers, J. Catal. 158 (1996) 551–560.
[6] F. Jousse, L. Leherte, D.P. Vercauteren, Mol. Simul. 17 (1996) 175–196.
[7] M.A. Asensi, A. Corma, A. Martinez, J. Catal. 158 (1996) 561–569.
[8] M. Trombetta, G. Busca, S. Rossini, V. Piccoli, U. Cornaro, J. Catal. 168 (1997) 349–363.
[9] P. Andy, N.S. Gnep, M. Guisnet, E. Benazzi, C. Travers, J. Catal. 173 (1998) 322–332.
[10] J. Houzvicka, S. Hansildaar, V. Ponec, J. Catal. 167 (1997) 273–278.
[11] F. Jousse, L. Leherte, D.P. Vercauteren, J. Mol. Catal. 119 (1997) 165–176.
[12] G. Onyestyak, J. Valyon, G. Pal-Borbely, L.V.C. Rees, Appl. Surf. Sci. 196 (2002) 401–407.
[13] P. Ivanov, H. Papp, Langmuir 16 (2000) 7769–7772.
[14] R. Byggningsbacka, N. Kumar, L.E. Lindfors, J. Catal. 178 (1998) 611–620.
[15] C. Paze, B. Sazak, A. Zecchina, J. Dwyer, J. Phys. Chem. B 103 (1999) 9978–9986.
[16] I.D. Harrison, H.F. Leach, D.A. Whan, Zeolites 7 (1987) 21–27.
[17] J.N. Kondo, K. Domen, J. Mol. Catal. 199 (2003) 27–38.
[18] S.-H. Lee, C.-H. Shin, S.B. Hong, J. Catal. 223 (2004) 200–211.
[19] A.G. Gayubo, A.T. Aguayo, A.E.S. del Campo, Ind. Eng. Chem. Res. 39 (2000) 292–300.
[20] J. Sommer, R. Jost, M. Hachoumy, Catal. Today 38 (1997) 309–319.
[21] M.V. Frash, R.A. van Santen, Top. Catal. 9 (1999) 191–205.
[22] J. Cejka, A. Vondrova, B. Wichterlova, Zeolites 14 (1994) 147–153.
[23] F. Cavani, F. Trifiro, G. Giordano, Appl. Catal. A 94 (1993) 131–152.
[24] A.K. El Morsi, S.A. Shokry, Petrol. Sci. Technol. 18 (2000) 1195–1207.
[25] S. Namuangruk, P. Pantu, J. Limtrakul, J. Catal. 225 (2004) 523–530.
[26] S. Kasuriya, S. Namuangruk, P. Treesukol, M. Tirtowidjojo, J. Limtrakul, J. Catal. 219 (2003) 320–328.
[27] W. Panjan, J. Limtrakul, J. Mol. Struct. 654 (2003) 35–45.
[28] C. Raksakoon, J. Limtrakul, J. Mol. Struct. 631 (2003) 147–156.
[29] A. Pelmenschikov, J. Leszczynski, J. Phys. Chem. B 103 (1999) 6886–6890.
[30] T.A. Wesolowski, O. Parisel, Y. Ellinger, J. Weber, J. Phys. Chem. A 101 (1997) 7818–7825.
[31] E.G. Derouane, C.D. Chang, Microporous Mesoporous Mater. 35–36 (2000) 425–433.
[32] L.A. Clark, M. Sierka, J. Sauer, Stud. Surf. Sci. Catal. 142A (2002) 643–649.
[33] X. Rozanska, R.A. van Santen, T. Demuth, F. Hutschka, J. Hafner, J. Phys. Chem. B 107 (2003) 1309–1315.
[34] F. Maseras, K. Morokuma, J. Comp. Chem. 16 (1995) 1170–1179.
[35] A.K. Rappe, C.J. Casewit, K.S. Colwell, W.A. Goddard, W.M. Skiff, J. Am. Chem. Soc. 114 (1992) 10024–10035.
[36] M.J. Frisch, G.W. Trucks, H.B. Schlegel, G.E. Scuseria, M.A. Robb, J.R. Cheeseman, J.A. Montgomery Jr., T. Vreven, K.N. Kudin, J.C. Burant, J.M. Millam, S.S. Iyengar, J. Tomasi, V. Barone, B. Mennucci, M. Cossi, G. Scalmani, N. Rega, G.A. Petersson, H. Nakatsuji, M. Hada, M. Ehara, K. Toyota, R. Fukuda, J. Hasegawa, M. Ishida, T. Nakajima, Y. Honda, O. Kitao, H. Nakai, M. Klene, X. Li, J.E. Knox, H.P. Hratchian, J.B. Cross, C. Adamo, J. Jaramillo, R. Gomperts, R.E. Stratmann, O. Yazyev, A.J. Austin, R. Cammi, C. Pomelli, J.W. Ochterski, P.Y. Ayala, K. Morokuma, G.A. Voth, P. Salvador, J.J. Dannenberg, V.G. Zakrzewski, S. Dapprich, A.D. Daniels, M.C. Strain, O. Farkas, D.K. Malick, A.D. Rabuck, K. Raghavachari, J.B. Foresman, J.V. Ortiz, Q. Cui, A.G. Baboul, S. Clifford, J. Cioslowski, B.B. Stefanov, G. Liu, A. Liashenko, P. Piskorz, I. Komaromi, R.L. Martin, D.J. Fox, T. Keith, M.A. Al-Laham, C.Y. Peng, A. Nanayakkara, M. Challacombe, P.M.W. Gill, B. Johnson, W. Chen, M.W. Wong, C. Gonzalez, J.A. Pople, Gaussian Inc., Pittsburgh, PA, 2003.
[37] A.E. Reed, L.A. Curtiss, F. Weinhold, Chem. Rev. 88 (1988) 899–926.

[38] J. Klinowski, Chem. Rev. 91 (1991) 1459–1479.

[39] D.W.F. Brilman, W.P.M. van Swaaij, G.F. Versteeg, Ind. Eng. Chem. Res. 36 (1997) 4638–4650.

[40] F. Tielens, J.F.M. Denayer, I. Daems, G.V. Baron, W.J. Mortier, P. Geerlings, J. Phys. Chem. B 107 (2003) 11065–11071.

[41] M. Boronat, C.M. Zicovich-Wilson, P. Viruela, A. Corma, J. Phys. Chem. B 105 (2001) 11169–11177.

[42] E.M. Evleth, E. Kassab, H. Jessri, M. Allavena, L. Montero, L.R. Sierra, J. Phys. Chem. 100 (1996) 11368–11374.

[43] S. Svelle, B. Arstad, S. Kolboe, O. Swang, J. Phys. Chem. B 107 (2003) 9281–9289.

[44] M. Boronat, P.M. Viruela, A. Corma, J. Am. Chem. Soc. 126 (2004) 3300–3309.

[45] E. Yoda, J.N. Kondo, K. Domen, J. Phys. Chem. B 109 (2005) 1464–1472.

[46] N.W. Cant, W.K. Hall, J. Catal. 25 (1972) 161–172.

[47] V. Nieminen, M. Sierka, D.Yu. Murzin, J. Sauer, J. Catal. 231 (2005) 393–404.